Article   **Open Access**

B$_4$C/g-C$_3$N$_4$ p-n Heterojunction with Enhanced Photoactivity for the Degradation of Aqueous Pollutants

Chenjing Sun, Ruishuo Li, Rui Wang

School of Environmental Science and Engineering, Shandong University, No. 72 Seaside Road, Jimo, Qingdao, 266237, PR China

Abstract

The novel p-n heterojunction B$_4$C/g-C$_3$N$_4$ photocatalysts were built via ultrasonic dispersion, and solvent evaporation approaches. The properties of the photocatalysts were studied by characterization. The photocatalytic performance of materials was investigated by degradation of Rhodamine B (RhB) and tetracycline (TC). The B$_4$C/g-C$_3$N$_4$ (1/6) showed the best photocatalytic performance for the degradation of RhB (96%, in 70 min). Its degradation rate was 32 % higher than that of single g-C$_3$N$_4$. Besides, 92% TC could be degraded by B$_4$C/g-C$_3$N$_4$ (1/6) in 210 min. Compared with the pure g-C$_3$N$_4$, the photocatalytic activity of the B$_4$C/g-C$_3$N$_4$ composites was improved significantly. On the one hand, the modification of B$_4$C enhanced the light absorption capacity. On the other hand, the formed p-n hetero-junction between B$_4$C and g-C$_3$N$_4$ enhanced the charge transfer rate and inhibited the recombination of photogenerated electrons and holes. Therefore, the composites could generate a lot of active species to degrade aqueous pollutants. In addition, the materials exhibited excellent stability in recycling tests. This study provides novel p-n heterojunction photocatalysts for degradation pollutants.

Keywords: *g-C$_3$N$_4$; B$_4$C; p-n heterojunction; photocatalysis; visible light.*

1. Introduction

Due to the high molecular weight, complex composition, carcinogenicity, teratogenicity, and other characteristics, refractory pollutants are seriously harmful to the environment and human beings [1-3]. It is of great significance to treat the refractory pollutants in water. Traditional methods for treating refractory pollutants, such as activated carbon adsorption and membrane treatment, have the disadvantages of low mineralization, low efficiency, and low economic benefits [4-5]. Therefore, new technologies and processes are urgently needed to treat refractory pollutants. Nowadays, photocatalytic technology has gained more and more attention in the treatment of refractory pollutants due to its energy-saving properties, complete mineralization, no secondary pollution, and simple operation [6-8]. As the traditional semiconductor photocatalyst, titanium dioxide (TiO$_2$) exhibits obvious limitations in the degradation of pollutants due to its wide bandgap and low light absorption capacity. Thus, the development of photocatalysts with suitable bandgap and high photocatalytic degradation performance has been the current research hotspot.

Recently, g-C$_3$N$_4$ as an inorganic non-metallic material has received great attention with its suitable bandgap, unique optical performance, and high stability [9-13]. However, the single g-C$_3$N$_4$ has the common shortcomings of photocatalysts: low utilization of visible light and high recombination rate of photogenerated carriers [14]. Hence, the photocatalytic performance of g-C$_3$N$_4$ needs to be further improved. The main improvement methods of g-C$_3$N$_4$ included element doping [15,16], heterojunction construction [17-20] and defect control [21-22]. Since g-C$_3$N$_4$ is a typical n-type photocatalyst, the construction of p-n type heterojunction is one of the primary methods to enhance the photocatalytic activity of g-C$_3$N$_4$ at all time. It can enhance the ability to absorb visible light and facilitate the charge transfer of g-C$_3$N$_4$ by building p-n

heterojunction. For example, Liang *et al.* synthesized $LaFeO_3$/g-C_3N_4 p-n heterojunction photocatalyst, which exhibited much higher photocatalytic performance for RhB degradation compared to the bare g-C_3N_4 [23]. Guo *et al.* verified that $CuBi_2O_4$/g-C_3N_4 p-n heterojunctions showed high photocatalytic performance in the degradation of TC [24]. Therefore, it is desirable to explore the suitable p-type photocatalysts to construct p-n heterojunction with high photocatalytic activity.

As a kind of P-type photocatalysts, boron carbide (B_4C) has gained more attention from researchers. On the one hand, B_4C exhibited excellent light absorption performance for the visible light due to its midgap states and structural relaxation [25]. On the other hand, the p-type characters of B_4C made it suitable to form p-n heterojunction, which can accelerate charge transfer and improve the photocatalytic performance [26]. Besides, B_4C also has the advantages of good stability, wild sources, and simple synthesis process [27]. In recent, B_4C/TiO_2 p-n heterojunction photocatalyst has been prepared successfully and showed an excellent photocatalytic performance in the production of CH_4 [28]. Herein, it is looking forward to enhancing the photocatalytic performance of g-C_3N_4 via building B_4C/g-C_3N_4 p-n heterojunctions, which might extend the light response range and reduce the recombination of photogenerated electrons and holes.

In this paper, B_4C/g-C_3N_4 p-n heterojunction photocatalysts were prepared by a simple method. The photocatalytic activities of samples were studied by degradation of RhB and TC under visible light irradiation. The tests showed that B_4C/g-C_3N_4 photocatalysts had better degradation ability to RhB and TC than single g-C_3N_4. Moreover, active species in the degradation process was determined by the scavenger experiment. According to the references, photoluminescence (PL) characterization, and experiment results, the possible photocatalytic mechanism for RhB degradation was inferred.

2. Experimental section

2.1. Materials

Urea was obtained from Bodi (Tianjin, China). Boron carbide was purchased from Shandong West Asia Chemical Industry Co., Ltd. Triethanolamine (TEOA) and concentrated nitric acid were procured from Fuyu (Tianjin, China). 1,4-benzoquinone(PBQ) was obtained from Shanghai Macklin Biochemical Co. Ltd. Rhodamine B and *tert*-butanol(TBA) were available from Kemiou (Tianjin, China). Tetracycline hydrochloride was procured from Shanghai Ruiyong Biotechnology Co., Ltd.

2.2. Synthesis of the photocatalysts

Synthesis of g-C_3N_4: The g-C_3N_4 was synthesized by the typical calcination method [29]. Briefly, 20.0 g urea was placed into a quartz boat and heated to 550°C for 3 h with a heating rate of 3.5°C/min in the tube furnace. After cooling to room temperature, the yellow product was taken out and grounded into powder with an agate mortar.

Synthesis of B_4C/g-C_3N_4 composites: Before using B_4C, it needed to be purified and washed with dilute hydrochloric acid and water for several times to remove the possible impurities. The B_4C/g-C_3N_4 composites were synthesized via gentle solvent evaporation ways. Firstly, the appropriate amount of g-C_3N_4 was dispersed to 30mL of water and treated by ultrasonic wave (29 kHz) for 720 min. Then a certain amount of B_4C was added to the solution and continued to be treated by ultrasonic wave (29 KHz) for 120 min. After the materials were uniformly dispersed, the solution was put into 90°C water bath and stirred to evaporate the solvent. Lastly, the resultant products were dried in a vacuum oven at 120°C.

2.3. Characterization

X-ray diffraction (XRD) patterns of samples were performed by Bruker D8 ADVANCE instrument using Cu-Kα radiation. The emission scanning electron microscopy (SEM) images were characterized by the JSM-6700 (Hitachi, Japan). The optical characteristics of samples were

determined by UV–vis diffuse reflectance spectra (SHIMADZU, UV-2550). Photoluminescence (PL) spectroscopy was characterized by F-4500 fluorescence spectrophotometer (Hitachi, Japan).

2.4. Photocatalytic activities

In order to verify the photocatalytic activity of B_4C/g-C_3N_4 composites for degradation of the refractory pollutants, RhB and TC were selected as target pollutants. The photocatalytic experiments were carried out as follows: 50 mg photocatalysts were added into 100 mL RhB solution (10mg/L) or 100 ml TC solution (20 mg/L), then the mixture was treated by ultrasonic wave for 5 min and stirred for 30 min in the dark to reach the adsorption-desorption equilibrium. Under stirring, the solution was irradiated by a 300W-Xeon lamp equipped with a 420 nm cut-off filter. During the reaction, 3 ml of the suspension was extracted at a certain time interval and centrifuged at 1000 r/min for 10 min to separate photocatalyst. The concentrations of supernatants were determined by UV–vis spectrophotometer (SP-756PC, China). In determining stability test, the photocatalysts were collected by centrifugation, rinsed alternately with ethanol and deionized water, dried at 70 °C, and then used in the next repeated experiment.

3. Results and discussions

3.1. Characterization of photocatalysts

The crystalline phases of prepared photocatalysts were determined by XRD. As shown in Fig.1, the two typical peaks at 13.1° and 27.7° of single g-C_3N_4 were related well to the pure g-C_3N_4 (JPCDS No. 87-1526).
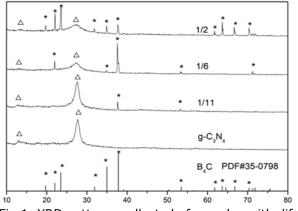

Fig.1. XRD patterns collected of samples with different mass ratios

The characteristic peaks at 13.1°, 19.8°, 21.6°, 22.9°, 27.7°, 32.1°, 35.3°, and 37.9° of B_4C/g-C_3N_4 composites were in good agreement with the pure g-C_3N_4 (JPCDS No. 87-1526) and B_4C (JPCDS No.35-0798). With the increasing content of B_4C in B_4C/g-C_3N_4 p-n heterojunction composites, the peak intensity of g-C_3N_4 was decreased, while the peak intensity of B_4C was increased. Besides, there were no other characteristic peaks in the composites. The results showed that B_4C and g-C_3N_4 were successfully combined.
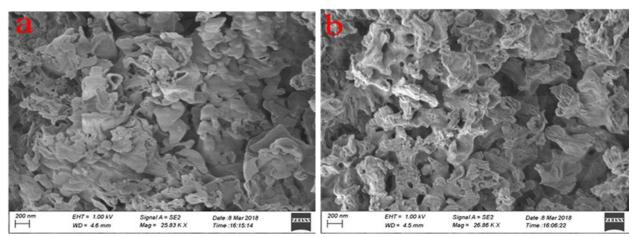

Fig.2. SEM patterns of (a) g-C_3N_4 and (b) B_4C/g-C_3N_4(1/6)

The morphologies of the single g-C_3N_4 and B_4C/g-C_3N_4 (1/6) composite were exhibited via SEM analysis. From Fig.2a, it can be seen that single g-C_3N_4 showed slate-like and aggregated layers with a smooth structure. After combining B_4C, the surface of composites became un-smooth, and B_4C particles were embedded and dispersed on the surface of g-C_3N_4 nanosheets (Fig.2b). It indicated that B_4C/g-C_3N_4 heterojunction was successfully synthesized by solvent evaporation approach.
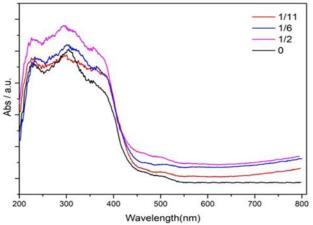

Fig.3. UV–vis spectrums of as-prepared photocatalysts

The UV-vis diffuse reflectance spectroscopy (DRS) was used to investigate the optical properties of photocatalysts. As shown in Fig.3, the absorption band edge of g-C_3N_4 was extended up to 450 nm, which showed that the pure g-C_3N_4 could respond to the visible light. When the mass ratio of B_4C was increased, the absorption edge of B_4C/g-C_3N_4 photocatalysts occurred red-shift. It implied that the modification of B_4C enhanced the light absorption ability of g-C_3N_4. Thus, B_4C/g-C_3N_4 composites could generate more carriers to participate in the photocatalytic reaction under visible light irradiation.

In order to study the transfer of photogenerated carriers, the photoluminescence (PL) spectra were characterized. It is universally acknowledged that the lower intensity of PL spectra reveals the lower recombination rate of photogenerated electron-hole pairs [30].
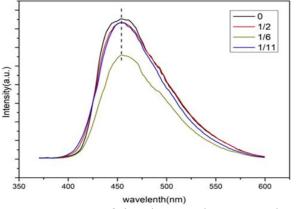

Fig.4. PL spectra of the photocatalysts excited at the wavelength of 325 nm

Fig.4 displayed the PL spectra of g-C_3N_4 and B_4C/g-C_3N_4 composites with different mass ratios. It can be discovered that the photoluminescence intensity of single g-C_3N_4 was higher than that of all B_4C/g-C_3N_4 samples, indicating that the recombination rate of photogenerated electron-hole pairs was reduced after combining B_4C. Besides, B_4C/g-C_3N_4 (1/6) composite exhibited the lowest PL intensity among all materials. The result was mainly caused by the formed p-n heterojunction between B_4C and g-C_3N_4, which can accelerate the transfer of excited carriers and prolong the lifetime of un-paired holes and electrons.

3.2. Photocatalytic activity and stability

The photocatalytic activity of prepared samples was investigated by the degradation of RhB under visible light. As shown in Fig.5, B_4C/g-C_3N_4 p-n heterojunction photocatalysts showed higher photocatalytic activities than the single g-C_3N_4. With the increasing contents of B_4C, the photocatalytic efficiency of B_4C/g-C_3N_4 materials increased at first and then decreased. B_4C/g-C_3N_4 (1/6) showed the best performance for the degradation of RhB among composites. The photocatalytic degradation rate reached 96% in 70 min, which was approximately 32% higher than that of single C_3N_4. The results were assigned to the formation of a built-in electric field between composites, which could promote the separation of photogenerated electron-hole pairs and effectively suppress the recombination of carriers. Therefore, more active species could react with the contaminants to improve the photocatalytic degradation rate. Once the mass ratio of B_4C to g/C_3N_4 exceeded 1/6, the excess B_4C is easy to aggregate. Since no more efficient heterojunction was formed, the degradation rate described a decreasing trend.

Through studying the kinetics of the reaction process, the RhB degradation process was suitable for the pseudo-first-order kinetics:

$$-ln(C/C_0) = kt \tag{1}$$

where C and C_0 are the initial and timely concentrations of RhB, respectively and k is the first-order rate constant.

As shown in Fig.6, the rate constant k for RhB degradation over $B_4C/g\text{-}C_3N_4$ (1/6) was 0.014, which was almost 3.5 times higher than that of bare $g\text{-}C_3N_4$. These results showed that $B_4C/g\text{-}C_3N_4$ (1/6) had excellent photocatalytic performance under visible light.
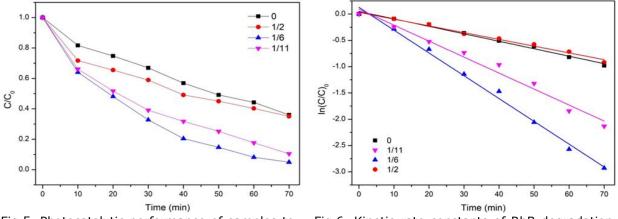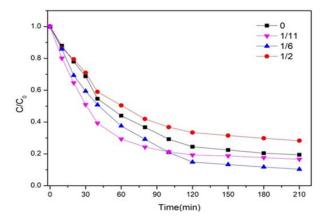

Fig.5. Photocatalytic performance of samples towards the degradation of RhB

Fig.6. Kinetic rate constants of RhB degradation over $B_4C/g\text{-}C_3N_4$ composites

In addition, the degradation of TC as a colorless pollutant was also investigated to determine the photocatalytic activity of prepared composites. As shown in Fig.7, the result was in accordance with the degradation of RhB. $B_4C/g\text{-}C_3N_4$ (1/6) showed the best performance of the degradation of TC, and the photocatalytic degradation rate reached 92% in 210 min. Based on the above experiments, the excellent photocatalytic performance of $B_4C/g\text{-}C_3N_4$ composites was confirmed.

Stability is also important to evaluate the performance of photocatalyst. The repeated experiments were carried out with photocatalysts collected after the photodegradation experiment. From Fig.8, it can be found that the photocatalytic activity of $B_4C/g\text{-}C_3N_4$ (1/6) had only a slightly descend after four repeated experiments for photocatalytic degradation of RhB. It might be due to the inevitable wastage of photocatalyst in the recovery process. The results testified that the $B_4C/g\text{-}C_3N_4$ (1/6) showed excellent photocatalytic performance and stability.
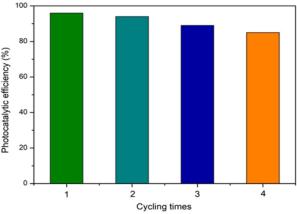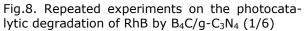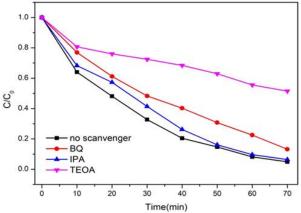

Fig.7. Photocatalytic performance of samples towards the degradation of TC

Fig.8. Repeated experiments on the photocatalytic degradation of RhB by $B_4C/g\text{-}C_3N_4$ (1/6)

3.3. Possible mechanism of photocatalytic degradation

In order to verify the main active species in the photocatalytic reaction, the trapping experiments in the RhB degradation process were carried out. In the experiment, 10 mM/L p-Benzoquinone (p-BQ), isopropanol (IPA), or triethanolamine (TEOA) were added into the RhB solution as superoxide radical ($\cdot O^{2-}$), scavenger hydroxyl radical ($\cdot OH$) and holes (h^+) scavenger, respectively. As shown in Fig.9, the degradation efficiency of RhB was 86% after adding p-BQ, the degradation rate of RhB even decreased to 49% after adding TEOA, while the degradation efficiency of RhB still reached 93% after adding IPA. The results demonstrated that h^+ was the main active species in the photocatalytic process of $B_4C/g-C_3N_4(1/6)$. The relative effect of $\cdot O^{2-}$ was second, while $\cdot OH$ was not the main active species in the photocatalytic process.
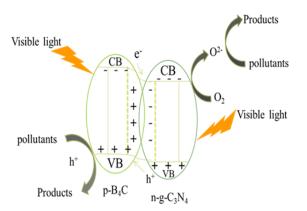

Fig.9. Trapping experiment of active species during the photocatalytic degradation of RhB

Fig.10. Possible photocatalytic mechanism over $B_4C/g-C_3N_4$ under visible light irradiation

Based on the above results and references, the possible mechanism of degrading contaminants by $B_4C/g-C_3N_4$ p-n heterojunction was speculated. As shown in Fig.10, the B_4C and $g-C_3N_4$ could be both excited under visible light. Firstly, the generated electrons would transfer to their respective conduction band (CB), while the generated holes would remain in their respective valence band (VB). Because the CB of B_4C was higher than that of $g-C_3N_4$ in the formed p-n heterojunction, the electrons in the CB of B_4C would migrate to the CB of $g-C_3N_4$; Similarly, the VB of $g-C_3N_4$ was higher than that of B_4C, so the holes in the VB of $g-C_3N_4$ would transfer to the VB of B_4C and directly participate in the degradation of pollutants. Therefore, the formation of p-n heterojunction in $B_4C/g-C_3N_4$ composites can accelerate the charge transfer and generate more active species to improve the photocatalytic activity.

4. Conclusion

In summary, the novel $B_4C/g-C_3N_4$ p-n heterojunction composites were successfully prepared. The photocatalytic experiments demonstrated that $B_4C/g-C_3N_4$ (1/6) showed optimum photocatalytic activity. The degradation efficiency of RhB reached 96% in 70 min, and that of TC was 92 % in 210 min. The outstanding stability of photocatalysts was verified by the recycling experiment. The characterization results indicated that excellent photocatalytic performance might be attributed to the enhancement of light absorption capacity. More importantly, the built-in electron field constructed by p-n heterojunction could improve the photogenerated carriers transfer and reduce the recombination of photogenerated electron-hole pairs. Thus a lot of active species could be generated to participate in the photocatalytic reaction. Radical scavenger experiments verified that h^+ played a major role in photocatalytic degradation. This study indicated that building p-n heterojunctions between B_4C and $g-C_3N_4$ may be a promising method for improving photocatalytic performance.

Acknowledgments

References

[1] Kaushik P, Malik A. Fungal dye decolourization: recent advances and future potential. Environ. Int., 2009; 35:127-141.

[2] Eng D, Guo J, Zeng G, Sum G. Decolorization of anthraquinone，triphenylmethane and azo dyes by a new isolated Bacillus cereus strain DC11. Int. Biodeterior. Biodegrad., 2008; 62: 263-269.

[3] Peterson J W, Gu B, Seymour M D. Surface interactions and degradation of a fluoroquinolone antibiotic in the dark in aqueous TiO_2 suspensions. Sci. Total Environ., 2015; 532: 398-403.

[4] Thamaraiselvan C, Noel M. Membrane processes for dye wastewater treatment: recent progress in fouling control. Crit. Rev. Environ. Sci. Technol., 2015; 45(10): 1007-1040.

[5] Hameed B H, Din A T M, Ahmad A L. Adsorption of methylene blue onto bamboo-based activated carbon: kinetics and equilibrium studies. J. Hazard. Mater., 2007; 141(3): 819-825.

[6] Zhang J, Chen Y, Wang X. Two-dimensional covalent carbon nitride nanosheets: synthesis, functionalization, and applications. Energy Environ. Sci., 2015; 8: 3092–3108.

[7] Reddy P A K, Reddy P V L, Kwon E, Kim K H, Akter T, Kalagara S. Recent advances in photocatalytic treatment of pollutants in aqueous media. Environ. Int., 2016; 91: 94-103.

[8] Xiao J, Xie Y, Gao H, Wang Y, Zhao Z. g-C_3N_4–triggered super synergy between photocatalysis and ozonation attributed to promoted OH generation. Catal. Commun., 2015; 66: 10-14.

[9] Ong W J, Tan L L, Ng Y H, Yong S T, Chai S P. Graphitic carbon nitride (g-C_3N_4)-based photocatalysts for artificial photosynthesis and environmental remediation: are we a step closer to achieving sustainability? Chem. Rev., 2016; 116: 7159–7329.

[10] Wen J Q, Xie J, Chen X B, Li X. A review on g-C_3N_4-based photocatalysts. Appl. Surf. Sci., 2017; 391: 72-123.

[11] Zhang C, Li Y, Shuai D, Shen Y, Xiong W, Wang L. Graphitic carbon nitride (g-C_3N_4)-based photocatalysts for water disinfection and microbial control: A review. Chemosphere, 2019; 214: 462-479.

[12] Ren Y, Zeng D, Ong W J. Interfacial engineering of graphitic carbon nitride (g-C_3N_4)-based metal sulfide heterojunction photocatalysts for energy conversion: a review. Chin. J. Catal., 2019; 40(3): 289-319.

[13] Lam S M, Sin J C, Mohamed A R. A review on photocatalytic application of g-C_3N_4/semiconductor (CNS) nanocomposites towards the erasure of dyeing wastewater. Mater. Sci. Semicond. Process, 2016; 47: 62-84.

[14] Cao S, Low J, Yu J, Jaroniec M. Polymeric photocatalysts based on graphitic carbon nitride. Adv. Mater., 2015; 27(13): 2150-2176.

[15] Kong J Z, Zhai H F, Zhang W, Wang S S, Zhao X R, Li M, Wu D. Visible light-driven photocatalytic performance of N-doped ZnO/g-C_3N_4 nanocomposites. Nanoscale Res. Lett., 2017; 12(1): 526.

[16] Deng P, Xiong J, Lei S, Wang W, Qu X, Xu Y, Cheng B. Nickel formate induced high-level in situ Ni-doping of g-C_3N_4 for a tunable band structure and enhanced photocatalytic performance. J. Mater. Chem. A., 2019; 7(39): 22385-22397.

[17] Mohamed N A, Ullah H, Safaei J, Ismail A F, Soth M F, Mat Teridi M A. Efficient Photoelectrochemical Performance of γ Irradiated g-C_3N_4 and Its g-C_3N_4@ $BiVO_4$ Heterojunction for Solar Water Splitting. J. Phys. Chem. C., 2019; 123(14): 9013-9026.

[18] Tang J, Guo R, Zhou W, Huang C, Pan W. Ball-flower like NiO/g-C_3N_4 heterojunction for efficient visible light photocatalytic CO_2 reduction. Appl. Catal., B. 2018; 237: 802-810.

[19] Fu J, Yu J, Jiang C, Cheng B. g-C_3N_4-Based heterostructured photocatalysts. Adv. Energy Mater., 2018; 8(3): 1701503.

[20] Jiang D, Zhu J, Chen M, Xie J. Highly efficient heterojunction photocatalyst based on nanoporous g-C_3N_4 sheets modified by Ag_3PO_4 nanoparticles: Synthesis and enhanced photocatalytic activity. J. Colloid Interface Sci., 2014; 417: 115-120.

[21] Ruan D, Kim S, Fujitsuka M, Majima T. Defects rich g-C_3N_4 with mesoporous structure for efficient photocatalytic H_2 production under visible light irradiation. Appl. Catal. B., 2018; 238: 638-646.

[22] Zhang Y, Shen C, Lu X, Mu X, Song P. Effects of defects in g-C_3N_4 on excited-state charge distribution and transfer: Potential for improved photocatalysis. Spectrochim. Acta, Part A., 2019: 117687.

[23] Liang Q, Jin J, Liu C, Xu S, Li Z. Constructing a novel pn heterojunction photocatalyst La-FeO_3/g-C_3N_4 with enhanced visible-light-driven photocatalytic activity. J. Alloys Compd., 2017; 709: 542-548.

[24] Guo F, Shi W, Wang H, Huang H, Liu Y, Kang Z. Fabrication of a $CuBi_2O_4$/g-C_3N_4 p–n hetero-junction with enhanced visible light photocatalytic efficiency toward tetracycline degradation. Inorg. Chem. Front., 2017; 4(10): 1714-1720.

[25] Yan D, Liu J, Fu X, Liu P, Luo H A, Low-temperature synthesis of mesoporous boron carbides as metal-free photocatalysts for enhanced CO_2 reduction and generation of hydroxyl radicals. J. Mater. Sci., 2019; 54(8): 6151-6163.

[26] Werheit H, Rotter H W, Shalamberidze S, Leithe-Jasper A, Tanaka T. Gapstate related pho-toluminescence in boron carbide. Phys. Status Solidi (b), 2011; 248:1275–1279.

[27] Liu J K, Wen S H, Hou Y, Zuo F, Beran G, Feng PY. Boron carbides as efficient, metal-free, visible-light-responsive photocatalysts. Angew. Chem. Int. Ed., 2013; 52: 3241–3245.

[28] Zhang X, Yang J, Cai T, Zuo G, Tang C. TiO_2 nanosheets decorated with B_4C nanoparticles as photocatalysts for solar fuel production under visible light irradiation. Appl. Surf. Sci., 2018;443: 558-566.

[29] Liu J, Zhang T, Wang Z, Dawson G, Chen W. Simple pyrolysis of urea into graphitic carbon nitride with recyclable adsorption and photocatalytic activity. J. Mater. Chem., 2011; 38: 14398-14401.

[30] Jing L Q, Qu Y C, Wang B Q, Li S D, Jiang B J, Yang L B, Fu W, Fu H G, Sun J Z. Review of photoluminescence performance of nano-sized semiconductor materials and its relationships with photocatalytic activity. Sol. Energy Mater. Sol. Cells., 2006; 90: 1773–1787.

To whom correspondence should be addressed: Dr. Wang Rui, School of Environmental Science and Engineering, Shandong University, No. 72 Seaside Road, Jimo, Qingdao, 266237, PR China E-mail wangrui@sdu.edu.cn